

# Analytical Theory of Second Harmonic Generation from a Nanoparticle with a Non-Centrosymmetric Geometry

Raksha Singla and W. Luis Mochán

*Instituto de Ciencias Físicas, Universidad Nacional Autónoma de México,*

*Apartado Postal 48-3, 62251 Cuernavaca, Morelos, México*

## Abstract

We analytically investigate the effect of a non-centrosymmetric geometry in the optical second harmonic (SH) generation from a particle made of a centrosymmetric material, in the interior of which quadratic optical processes are suppressed. We consider a cylindrical particle with a cross-section that is slightly deformed away from a circle and with a radius much smaller than the wavelength. We calculate the induced linear and nonlinear fields perturbatively in terms of the deformation parameter and obtain the nonlinear dipolar and quadrupolar hyperpolarizabilities, whose spectra we evaluate for metallic and dielectric materials. We show that for very small deformations the dipolar contribution to the response competes with the quadrupolar term, and may even be dominant. We explore the spectra of the hyperpolarizability and identify the contributions to its structure for metallic and dielectric particles. We also discuss the nature of SH radiation at various frequencies and find that it may be dominated by the dipolar or the quadrupolar term, or that both may compete yielding non-symmetric radiation patterns. Our calculation may be employed to assess, calibrate and test numerical SH calculations.

## I. INTRODUCTION

In recent years, the availability of novel techniques to produce nanoparticles with different shapes has attracted much attention as they can be engineered to exhibit unique nonlinear optical properties which are sensitive to their environment as well as their morphologies<sup>1,2</sup>. Exploring second harmonic generation (SHG) from nanoparticles and nanostructures has proven to be an extraordinary tool to probe the properties of their surfaces and interfaces. The surface sensitivity of the SH signal is due to the fact that the bulk signal is strongly suppressed within centrosymmetric systems; within the electric dipolar approximation, SHG from a centrosymmetric system takes place only at the surface as the bulk contribution is forbidden due to symmetry. The surface would also be expected to dominate the SHG from nanoparticles made of centrosymmetric materials, but if they possess a centrosymmetrical shape there would be a cancellation of the surface contributions to the nonlinear electrical dipole moment arising from opposite sides, leaving only quadrupolar and higher moments. However, when subjected to a nonuniform polarizing field, a symmetrical particle can generate SH due to the contributions arising from the excitation of a nonlocal dipole moment<sup>3-5</sup>. On the other hand, a homogeneous external field would generate a nonvanishing dipolar SH response even from nanoparticles made of centrosymmetric material if their geometry is non-centrosymmetric. SHG from nanoparticles, arrays of nanoparticles and nanostructured materials with a variety of geometries have been demonstrated experimentally and with supporting numerical<sup>6-10</sup> investigations. Several theoretical models have been reported in the past to study SH scattering in the Rayleigh limit from small symmetrical nanoparticles<sup>11,12</sup> or particles of arbitrary size<sup>13,14</sup> to include the effects of retardation and to explore SHG within the framework of Mie theory. An implementation of the discrete dipole approximation (DDA) model to explore SHG from small nanoparticles of various kinds was employed to study the influence of their shapes and sizes on their nonlinear optical properties<sup>15</sup>. Different studies involving various numerical computation techniques applied to diverse geometries have since then been reported. Some of them used the finite-difference time-domain (FDTD) method to investigate the SHG from nanoholes in a metal film<sup>10</sup>, and in particular, from an array of E shaped nanoholes within a metal film<sup>9</sup>. Others explored the effect of deformations of metallic spheres<sup>16</sup> on SHG using the finite element method (FEM). Investigation of SHG from gold split ring resonators<sup>17</sup> used different theoretical models and compared

their applicability. A surface integral approach was used to evaluate SH scattering from periodic metallic-dielectric nanostructure<sup>18</sup>, noble metal nanoparticles of arbitrary shape<sup>19,20</sup>, and gold nanorod and nanosphere<sup>21</sup>. Recently, a recursive method was employed to study the SH susceptibility, the tuning of its resonant structures and the corresponding nonlinear polarization within metamaterials made of an array of asymmetric cross shaped holes within metallic hosts<sup>22</sup>.

As illustrated by the studies mentioned above, most of the efforts to investigate SHG from nanoparticles have employed experimental or *numerical* methods. To the best of our knowledge, there have been no reports of an *analytical* calculation to study SHG from nanoparticles with a non-centrosymmetric geometry. The purpose of this paper is the calculation of the second order nonlinear response of an isolated nanoparticle made up of a centrosymmetric material with small deviations from a symmetrical geometry subjected to a homogeneous external field, obtaining and evaluating analytical expressions for the nonlinear dipolar and quadrupolar hyperpolarizabilities. We restrict our study to small deformations, which allows us to employ a perturbative scheme in order to be able to solve the field equations analytically for linear and SH induced fields within and beyond the surface of the nanoparticle. We consider the simplest geometry for which there is no centrosymmetry, namely, a cylinder having a slightly deformed, near circular cross-section with a threefold symmetry, and we use a nonretarded approximation to obtain the near fields which we use afterwards to calculate the electromagnetic fields in the radiation zone. We discuss the resonant structure of the nonlinear response for a model metal and a dielectric particle, the relation between the different components of the response tensor owing to the symmetry in the system and study the angular radiation patterns of the nanoparticle and their evolution as the frequency sweeps across the various resonances. As expected, we find the dipolar response to be highly dependent on the deformation parameter as a deviation of only 1% away from the symmetry of the shape of the particle results in a strong competition with the quadrupolar response.

The structure of the paper is the following. In Sec. II, we describe our theory to investigate analytically SHG from a deformed cylindrical particle, obtaining expressions for the nonlinear dipolar and quadrupolar hyperpolarizabilities (Sec. II A) and the SH radiation patterns (Sec. II B). Section III illustrates our results for a deformed cylinder made up of a Drude metal and a resonant dielectric. Finally, we present our conclusions in Sec. IV.

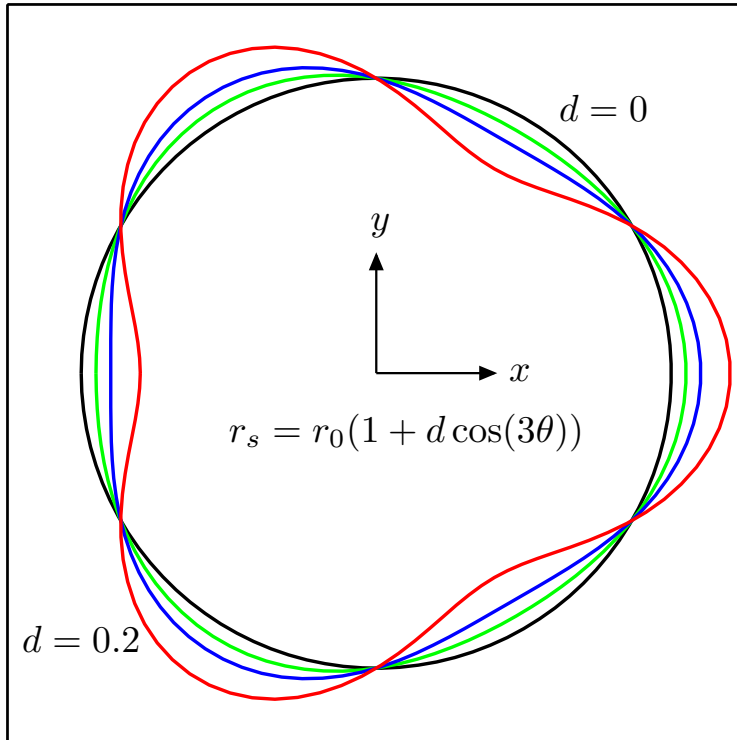


FIG. 1: Cross-section of a deformed cylinder described by Eq. (1) for various values of the deformation parameter  $d = 0.0 \dots 0.2$  (color online).

## II. NONLINEAR RESPONSE OF A DEFORMED CYLINDER

### A. Second order hyperpolarizabilities

We consider an isolated, infinitely long cylindrical particle placed in vacuum with its axis along the  $\hat{z}$  direction and a slightly deformed cross-section defined in polar  $(r, \theta)$  coordinates as

$$r_s(\theta) = r_0(1 + d \cos 3\theta) \quad (1)$$

(See Fig. 1) where  $r_0$  is the radius of a symmetric nominal circular cylinder and  $d$  is a small deformation parameter. We remark that we chose this geometry as it is the most simple one that lacks inversion geometry. Also note that our system possesses a mirror ( $y \rightarrow -y$ ) and a  $120^\circ$  rotational symmetry. We will study the nonlinear dipolar  $\mathbf{p}$  and quadrupolar  $\mathbf{Q}$  moments induced per unit length along the axis of the cylinder. We subject the particle to a homogeneous external electric  $\mathbf{E}^{\text{ex}}$  field oscillating at frequency  $\omega$ . Owing to the overall non-centrosymmetry of the geometry of the particle,  $\mathbf{p}$  has a local contribution proportional

to  $\mathbf{E}^{\text{ex}} \mathbf{E}^{\text{ex}}$  which we write as

$$p_i = \gamma_{ijk}^d E_j^{\text{ex}} E_k^{\text{ex}} \quad (2)$$

where  $\gamma_{ijk}^d$  is the dipolar hyperpolarizability and we use Einstein summation convention. Similarly, the induced quadratic 2D quadrupole moment, defined as

$$Q_{ij} = \int d^2r \rho(\mathbf{r})(2r_i r_j - r^2 \delta_{ij}) \quad (3)$$

(notice the difference with the usual 3D definition) is given by

$$Q_{ij} = \gamma_{ijkl}^Q E_k^{\text{ex}} E_l^{\text{ex}} \quad (4)$$

where  $\gamma_{ijkl}^Q$  is the quadrupolar hyperpolarizability. Here,  $\rho(\mathbf{r})$  is the 2D charge density.

For simplicity, we first assume that the external field is polarized along the  $\hat{\mathbf{x}}$  direction,  $\mathbf{E}^{\text{ex}} = E_0 \hat{\mathbf{x}}$ . Given the direction of the external field and the symmetries in the system, the only nonzero component of the nonlinear dipole moment induced in this case is  $p_x$ , which we write as

$$p_x = \gamma^d E_0^2. \quad (5)$$

in terms of a dipolar nonlinear response  $\gamma^d$  which is simply related all the components of the full dipolar hyperpolarizability  $\gamma_{ijk}^d$ . In this case the nonlinear quadrupole moment has only two nonzero components

$$Q_{xx} = -Q_{yy} = \gamma^Q E_0^2, \quad (6)$$

which we write in terms of a nonlinear response  $\gamma^Q$ , related to the full quadrupolar hyperpolarizability  $\gamma_{ijkl}^Q$ . In this section we calculate analytically  $\gamma^d$  and  $\gamma^Q$ .

In the nonretarded regime, the linear self-consistent near field may be obtained by solving Laplace's equation beyond and within the particle and applying boundary conditions at its interface. We start with the general solution of Laplace's equation outside

$$\phi_1^{\text{out}} = \phi^{\text{ex}} + \sum_{l=0}^{\infty} r^{-l} (s_l \cos l\theta + t_l \sin l\theta) \quad (7)$$

and within

$$\phi_1^{\text{in}} = \sum_{l=0}^{\infty} r^l (u_l \cos l\theta + v_l \sin l\theta), \quad (8)$$

the particle, with multipolar coefficients  $s_l$ ,  $t_l$ ,  $u_l$ , and  $v_l$  which we expand as power series on the deformation parameter  $d$

$$\beta_l = \sum_{n=0}^{\infty} \beta_l^{(n)} d^n, \quad (9)$$

where  $\phi^{\text{ex}} = -E_0 r \cos \theta$  is the external scalar potential and the generic coefficients  $\beta_l$  stand for any of  $s_l, t_l, u_l$  or  $v_l$ . In order to perform analytical calculations, we will restrict ourselves to small deformations and consider terms up to linear order in  $d$  only. Thus, solving Laplace's equation with appropriate boundary conditions<sup>23</sup> at the origin, the surface of the particle, and infinity, we obtain the self-consistent linear potential

$$\frac{\phi_1^{\text{out}}}{E_0} = r \cos \theta - \frac{1 - \epsilon_1}{1 + \epsilon_1} \frac{r_0^2}{r} \cos \theta - d \left[ \left( \frac{1 - \epsilon_1}{1 + \epsilon_1} \right)^2 \frac{r_0^3}{r^2} \cos 2\theta + \frac{1 - \epsilon_1}{1 + \epsilon_1} \frac{r_0^5}{r^4} \cos 4\theta \right], \quad (10)$$

$$\frac{\phi_1^{\text{in}}}{E_0} = \frac{2}{1 + \epsilon_1} r \cos \theta + 2d \frac{1 - \epsilon_1}{(1 + \epsilon_1)^2} \frac{r_0}{r^2} \cos 2\theta, \quad (11)$$

where  $\epsilon_g = \epsilon(g\omega)$  is the dielectric response of the particle at  $g$ -th harmonic frequency,  $g = 1, 2$ . From these results we may obtain the linear electric field  $\mathbf{E}_1$ .

The spatial variation of the self-consistent field within the particle induces a nonlinear polarization<sup>23</sup>

$$\mathbf{P}^{nl} = n\mathbf{p}^{nl} - \frac{1}{2}n\nabla \cdot \mathbf{q}^{nl}, \quad (12)$$

which includes contributions from the nonlinear dipole  $\mathbf{p}^{nl}$  and quadrupole  $\mathbf{q}^{nl}$  moments of each microscopic polarizable entity within the material, whose number density is  $n$ . Note that  $\mathbf{q}^{nl}$  may have a finite trace. Using the *dipolium* model<sup>24</sup>, we write

$$\mathbf{p}^{nl} = -\frac{1}{2e}\alpha_1\alpha_2\nabla E_1^2, \quad (13)$$

and

$$\mathbf{q}^{nl} = -\frac{1}{e}\alpha_1^2\mathbf{E}_1\mathbf{E}_1. \quad (14)$$

in terms of the linear electric field and the linear polarizability  $\alpha_g \equiv \alpha(g\omega)$  evaluated at the fundamental ( $g = 1$ ) and SH ( $g = 2$ ) frequencies, related to the dielectric function through  $\epsilon_g = 1 + 4\pi n\alpha_g$ .

The polarization, Eq. (12), yields a nonlinear bulk charge density given by

$$\rho^{nl} = -\nabla \cdot \mathbf{P}^{nl}, \quad (15)$$

which evaluates to zero up to linear order in  $d$  (it would be nonzero at order  $d^2$ ). The termination of the nonlinear polarization at the surface of the particle induces a nonlinear surface charge with density  $\sigma^b = \mathbf{P}^{nl}(r_s^-) \cdot \hat{\mathbf{n}}$  where  $\hat{\mathbf{n}}$  is a normalized outgoing vector perpendicular to the surface and  $r_s^- = r_s^-(\theta)$  denotes a position at the surface just inside

the particle. We employ the superindex  $b$  to denote the bulk origin of this surface charge. Using Eqs. (10) to (14) we identify

$$\sigma^b = 4d \frac{n}{er_0} \frac{(1 - \epsilon_1)}{(1 + \epsilon_1)^3} \alpha_1 (2\alpha_2 - \alpha_1) \cos \theta E_0^2. \quad (16)$$

As the inversion symmetry of the material is locally lost in a thin selvedge region around the surface, there is a nonlinear polarization induced at the surface of the particle which we write as

$$P_i^s = \chi_{ijk}^s F_j F_k, \quad (17)$$

where  $\chi_{ijk}^s$  are the components of the local nonlinear surface susceptibility and the field  $\mathbf{F}$  is defined in terms of quantities that are continuous across the surface to avoid the ambiguity about the position in the selvedge where the fields are to be calculated;  $\mathbf{F}$  is made up of the normal projection of the displacement field and the parallel projection of the electric field evaluated at the surface  $r_s(\theta)$ . Thus,

$$\mathbf{F}(r_s) = \mathbf{E}_1(r_s^+) = \epsilon_1 \mathbf{E}_1^\perp(r_s^-) + \mathbf{E}_1^\parallel(r_s^-), \quad (18)$$

where  $\mathbf{E}(r_s^-) = -\nabla\phi^{\text{in}}(r_s)$  and  $\mathbf{E}(r_s^+) = -\nabla\phi^{\text{out}}(r_s^+)$  and  $\perp$  and  $\parallel$  denote the projections normal and parallel to the surface.

We will assume that the thickness of the selvedge region is much smaller than the radius of the cylinder and thus, that the surface can be considered as locally flat. We will further assume *local* invariance under rotations around the surface normal. Hence, the surface susceptibility may be parametrized as

$$\chi_{ijk}^s = \frac{(\epsilon_1 - 1)^2}{64\pi^2 n e} \left( \delta_{i\perp} \delta_{j\perp} \delta_{k\perp} \frac{a}{\epsilon_1^2} + [(1 - \delta_{i\perp})(1 - \delta_{j\perp})\delta_{k\perp} + (1 - \delta_{i\perp})\delta_{j\perp}(1 - \delta_{k\perp})] \frac{b}{\epsilon_1} + \delta_{i\perp}(1 - \delta_{j\perp})(1 - \delta_{k\perp})f \right), \quad (19)$$

in a local reference frame where one of the cartesian directions is perpendicular and the others are parallel to the surface. Here,  $a$ ,  $b$ , and  $f$  are dimensionless functions of  $\omega$  used to parametrize the response of the surface<sup>25</sup> given in the *dipolium* model<sup>24</sup> by

$$a(\omega) = 2 \frac{(\epsilon_2 - \epsilon_1)(2\epsilon_1 - \epsilon_2 - \epsilon_1\epsilon_2) + \epsilon_1^2(1 - \epsilon_2) \log(\epsilon_1/\epsilon_2)}{(\epsilon_2 - \epsilon_1)^2}, \quad (20)$$

$$b = -1, \quad (21)$$

$$f = 0. \quad (22)$$

The normal component of the nonlinear polarization induced on the surface of the cylinder is obtained by substituting Eqs. (18) and (19) in Eq. (17),

$$P_{\perp}^s = \frac{1}{32\pi^2 ne} \left( \frac{1 - \epsilon_1}{1 + \epsilon_1} \right)^2 \left\{ (a + f) + (a - f) \cos 2\theta - d \left[ \left( 4 \frac{1 - \epsilon_1}{1 + \epsilon_1} + 3(a - f) \right) \cos \theta + 4 \frac{1 - \epsilon_1}{1 + \epsilon_1} \cos 3\theta - 3(a - f) \cos 5\theta \right] \right\} E_0^2. \quad (23)$$

The variation of the tangential component of the nonlinear surface polarization along the surface yields another contribution to the surface charge  $\sigma^s$  beyond that due to the termination of the bulk nonlinear polarization  $\sigma^b$ , where we use the superscript  $s$  to denote its surface origin. It is given by

$$\sigma^s = -\nabla_{\parallel} \cdot \mathbf{P}_{\parallel}^s, \quad (24)$$

where  $\nabla_{\parallel}$  is the gradient operator projected along the surface and  $\mathbf{P}_{\parallel}^s$  is the projection of  $\mathbf{P}^s$  along the surface. Substituting Eqs. (17) and (19) in Eq. (24) we obtain

$$\sigma^s = \frac{b}{8\pi^2 ner_0} \left( \frac{1 - \epsilon_1}{1 + \epsilon_1} \right)^2 \left[ \cos 2\theta + d \left( \cos \theta - 6 \frac{1 - \epsilon_1}{1 + \epsilon_1} \cos 3\theta + 7 \cos 5\theta \right) \right] E_0^2. \quad (25)$$

The screened scalar potential  $\phi_2$  induced at the SH frequency has  $\rho^{\text{nl}} (= 0)$  as an *external* bulk source and the total nonlinear charges induced at the surface  $\sigma^b$  and  $\sigma^s$  as external surface sources, together with the normal polarization  $P_{\perp}^s$ , which are accounted through the boundary conditions. The external sources have to be screened by the linear response of the particle at SH frequency  $\epsilon_2$ . Thus the equation to be solved for the quadratic scalar potential is

$$\nabla^2 \phi_2 = \begin{cases} 0 & (\text{outside}) \\ -4\pi \rho^{\text{nl}} / \epsilon_2 = 0 & (\text{inside}) \end{cases} \quad (26)$$

subject to the boundary conditions

$$\hat{\mathbf{n}} \cdot \nabla \phi_2(r_s^+) - \epsilon_2 \hat{\mathbf{n}} \cdot \nabla \phi_2(r_s^-) = -4\pi(\sigma^b + \sigma^s) \quad (27)$$

$$\phi_2(r_s^+) - \phi_2(r_s^-) = 4\pi P_{\perp}^s \quad (28)$$

Eq. (27) is the discontinuity of the normal component of the displacement field due to the presence of the nonlinear surface charge. Eq. (28) is the discontinuity of the scalar potential due to the presence of the normal nonlinear surface polarization  $P_{\perp}^s$  which is a dipole layer across the selvedge of the particle. Solving Laplace's equation perturbatively to obtain the



self-consistent scalar potential at the SH frequency with terms up to linear order in  $d$  we obtain on the outside

$$\begin{aligned} \frac{\phi_2^{\text{out}}}{E_0^2} = & \frac{d}{4\pi n e} \frac{(1 - \epsilon_1)^2}{(1 + \epsilon_2)(1 + \epsilon_1)^2} \left( 4 \frac{\epsilon_1 - 2\epsilon_2 + 1}{1 + \epsilon_1} + 2b \frac{1 + 3\epsilon_2}{1 + \epsilon_2} + \frac{\epsilon_2 (\epsilon_2 - 3)(a - f)}{2(1 + \epsilon_2)} \right. \\ & + \frac{\epsilon_2 (7\epsilon_1 - 1)f + (\epsilon_1 - 7)a}{2(1 + \epsilon_1)} \left. \right) \frac{r_0}{r} \cos \theta \\ & + \frac{1}{8\pi n e} \left( \frac{1 - \epsilon_1}{1 + \epsilon_1} \right)^2 \frac{\epsilon_2(a - f) + 2b}{1 + \epsilon_2} \frac{r_0^2}{r^2} \cos 2\theta + \dots \end{aligned} \quad (29)$$

where we only kept the dipolar and quadrupolar contributions, and neglected higher multipoles, all of which are at least of order  $d$ , as their contribution to the radiation fields would be insignificant for small particles, at least by a factor of order  $r_0/\lambda$ , with  $\lambda$  the wavelength.

Finally, we compare Eq. (29) to the general expression of the 2D scalar potential in polar coordinates, we identify the corresponding components of the multipolar moments, and from Eqs. (5) and (6) we obtain the dipolar

$$\begin{aligned} \gamma^d = & \frac{dr_0}{4\pi n e} \frac{(1 - \epsilon_1)^2}{(1 + \epsilon_2)(1 + \epsilon_1)^2} \left( 4 \frac{\epsilon_1 - 2\epsilon_2 + 1}{1 + \epsilon_1} \right. \\ & \left. + 2b \frac{1 + 3\epsilon_2}{1 + \epsilon_2} + \frac{\epsilon_2 (\epsilon_2 - 3)(a - f)}{2(1 + \epsilon_2)} + \frac{\epsilon_2 (7\epsilon_1 - 1)f + (\epsilon_1 - 7)a}{2(1 + \epsilon_1)} \right) \end{aligned} \quad (30)$$

and quadrupolar

$$\gamma^Q = \frac{r_0^2}{8\pi n e} \left( \frac{1 - \epsilon_1}{1 + \epsilon_1} \right)^2 \frac{\epsilon_2(a - f) + 2b}{1 + \epsilon_2} \quad (31)$$

nonlinear response functions.

To the lowest order in the deformation parameter,  $\gamma^d$  is proportional to  $d$ , and thus, as expected, the dipolar response would disappear for a centrosymmetric circular cross-section. On the other hand,  $\gamma^Q$  is a constant, with no contribution proportional to  $d$ , and therefore it coincides with the corresponding result for a cylinder of circular cross-section. The contributions arising from the bulk and the surface to the nonlinear hyperpolarizabilities can be easily identified as the latter are proportional to the surface parameters  $a$ ,  $b$ , and  $f$ . Thus,  $\gamma^d$  has both surface and bulk contributions, while  $\gamma^Q$  has only surface contributions. Both  $\gamma^d$  and  $\gamma^Q$  inherit the spectral structure of the surface parameters, namely, of  $a(\omega)$ , and also exhibit additional resonances corresponding to the excitation of surface plasmons or surface plasmon-polaritons at the fundamental and second harmonic frequencies, given by  $\epsilon_1 = -1$  and  $\epsilon_2 = -1$  respectively.

Above we have explicitly shown the calculation of the nonlinear response of the particle with the external field in the  $\hat{x}$  direction. One can similarly evaluate the response of the particle to the external field pointing in other directions. However, due to the mirror and the  $120^\circ$  rotation symmetry in our system, all the in-plane components of the dipolar hyperpolarizability are zero except for  $\gamma_{xyy}^d = \gamma_{yxy}^d = \gamma_{yyx}^d = -\gamma_{xxx}^d = -\gamma^d$ . We have verified these results by repeating the calculations above for external fields pointing along different directions. It turns out that given these symmetry related relations, the nonlinear dipole moment induced in the deformed cylinder rotates anticlockwise by an angle  $2\theta$  when the external electric field is rotated clockwise by  $\theta$  (see Fig. 2). The symmetry in our system leads to an isotropic quadrupolar response given by  $Q_{ij} = \gamma^Q(2E_i E_j - E^2 \delta_{ij})$ , the quadratic quadrupolar moment has a principal axis along the external field and the only non-null components of the quadrupolar hyperpolarizability are  $\gamma_{xxxx}^Q = -\gamma_{xxyy}^Q = -\gamma_{yyxx}^Q = \gamma_{yyyy}^Q = \gamma_Q$  and  $\gamma_{xyxy}^Q = \gamma_{yxxy}^Q = \gamma_{xyyx}^Q = \gamma_{yxyx}^Q = 2\gamma_Q$ . Thus, for this system our calculations of  $\gamma^d$  and  $\gamma^Q$  using an external field along  $\hat{x}$  are sufficient to obtain the full response response of the particle.

## B. SH radiation

Now we turn our attention towards the calculation of the SH angular radiation pattern. Following a procedure similar to the  $3D$  case, one can write down the expressions for the radiated electromagnetic fields in  $2D$  due to localized distributions of charges and currents. Using the vector potential from Eqs. (A.42) and (A.44) (see Appendix), we calculate the radiated electromagnetic fields.

$$\mathbf{B} = (1 + i)k^{3/2} \left( (\hat{\mathbf{r}} \times \mathbf{p}) - \frac{i}{4}k^2(\hat{\mathbf{r}} \times (\mathbf{Q} \cdot \hat{\mathbf{r}})) \right) e^{ikr} \sqrt{\frac{\pi}{r}}, \quad (32)$$

$$\mathbf{E} = \mathbf{B} \times \hat{\mathbf{r}}, \quad (33)$$

where  $k$  is the wavenumber and  $\hat{\mathbf{r}}$  is the unit vector in the direction of observation. The time averaged power radiated per unit angle  $\theta$  due to these radiated fields is

$$\frac{dP}{d\theta} = \frac{rc}{8\pi} \text{Re}[\mathbf{E} \times \mathbf{B}^*] \cdot \hat{\mathbf{r}}. \quad (34)$$

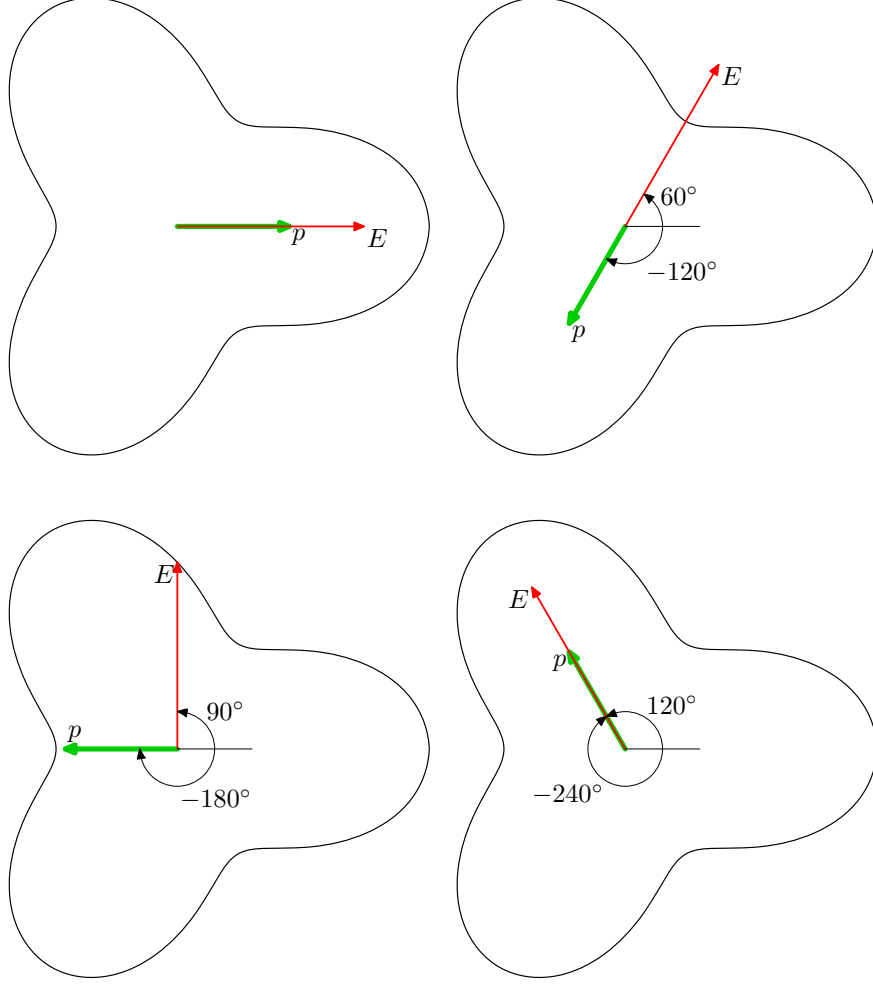


FIG. 2: Direction of the quadratic dipole moment induced in a deformed cylindrical particle by an external field with different directions with respect to the horizontal. As the field rotates clockwise by an angle  $\theta$  the dipole rotates counterclockwise by  $2\theta$  (color online).

From Eqs. (30) to (34) we obtain

$$\frac{dP}{d\theta} = \frac{cE_0^4 k^3}{4} \left( |\gamma^d|^2 \sin^2 \theta + 4k \operatorname{Im}(\gamma^d \gamma^{Q*}) \sin^2 \theta \cos \theta + 4k^2 |\gamma^Q|^2 \sin^2 \theta \cos^2 \theta \right). \quad (35)$$

The first and last terms correspond to dipolar and quadrupolar radiation, while the middle term corresponds to their interference.

### III. RESULTS

We consider a particle made up of a Drude metal characterized by its bulk plasma frequency  $\omega_p$  and electronic relaxation time  $\tau$ , with dielectric function  $\epsilon(\omega) = 1 - \omega_p^2/(\omega^2 + i\omega/\tau)$ <sup>26</sup>, with a small deformation parameter  $d = 0.01$  and with a small dissipation  $1/\omega_p\tau = 0.01$ . We remark that while the nonlinear dipolium model<sup>24</sup> corresponds to a continuous distribution of small polarizable entities, its results agree with those of a nonlinear local *jellium* with a continuous electronic density profile at the surface, and thus, it may be applied to metallic surfaces<sup>27</sup>. In Fig. 3 we show the absolute values and phases of the nonlinear dipolar and quadrupolar response functions  $\gamma^d$  and  $\gamma^Q$ . Notice that both display very large resonant peaks corresponding to the surface plasmon resonance of the cylinder  $\omega_{sp} = \omega_p/\sqrt{2}$  and to its subharmonic. Beyond abrupt changes at the resonances, the phase of  $\gamma^d$  shifts away from 0 in a wide region that spans from  $\omega_p/2$  up to  $\omega_p$ . This is due to the logarithm term in Eq. (20), whose argument changes sign as  $\omega$  or  $2\omega$  sweeps across the plasma frequency<sup>24</sup>. The phase of  $\gamma^Q$  also displays a smooth variation of around  $2\pi$  in the same region.

In Fig. 4 we show the absolute values and phases of  $\gamma^d$  and  $\gamma^Q$  for a similar deformed cylinder but made up of an insulator. We assume its dielectric function is dispersive and for simplicity we assume it has a single resonance described by a simple Lorentzian<sup>26</sup> form given by  $\epsilon(\omega) = (\omega_L^2 - \omega^2 - i\omega/\tau)/(\omega_T^2 - \omega^2 - i\omega/\tau)$  where  $\omega_L$  and  $\omega_T$  are the frequencies of the longitudinal and transverse optical modes respectively and included a very small dissipation characterized by  $\tau$ . For definitiveness, we took  $\omega_L = \sqrt{2}\omega_T$ . Both  $\gamma^d$  and  $\gamma^Q$  show strong resonant peaks corresponding to the excitation of the surface plasmon-polariton at  $\omega = \omega_{spp} = \omega_T\sqrt{3/2}$  and its subharmonic. The dielectric function crosses zero at  $\omega_L$  and has a pole at  $\omega_T = 1$ . The phase of both  $\gamma^d$  and  $\gamma^Q$  grows smoothly between  $\omega_T/2$  and  $\omega_L/2$ , and between  $\omega_T$  and  $\omega_L$ , save for abrupt jumps at  $\omega_{spp}/2$ ,  $\omega_T$  and  $\omega_{spp}$ , and remain constant otherwise. Some features in the phase of  $\gamma^d$  and  $\gamma^Q$  are inherited from those of the parameter  $a$ <sup>24</sup>.

In Fig. 5 we plot the pattern  $dP/d\theta$  vs. the polar angle  $\theta$  corresponding to a deformed metallic cylinder as that in Fig. 3, described by the Drude response and with a deformation parameter  $d = 0.01$ , illuminated by a TM electromagnetic wave propagating along the  $y$  axis with an electric field pointing along the  $x$  axis, assuming that the nominal radius  $r_0$

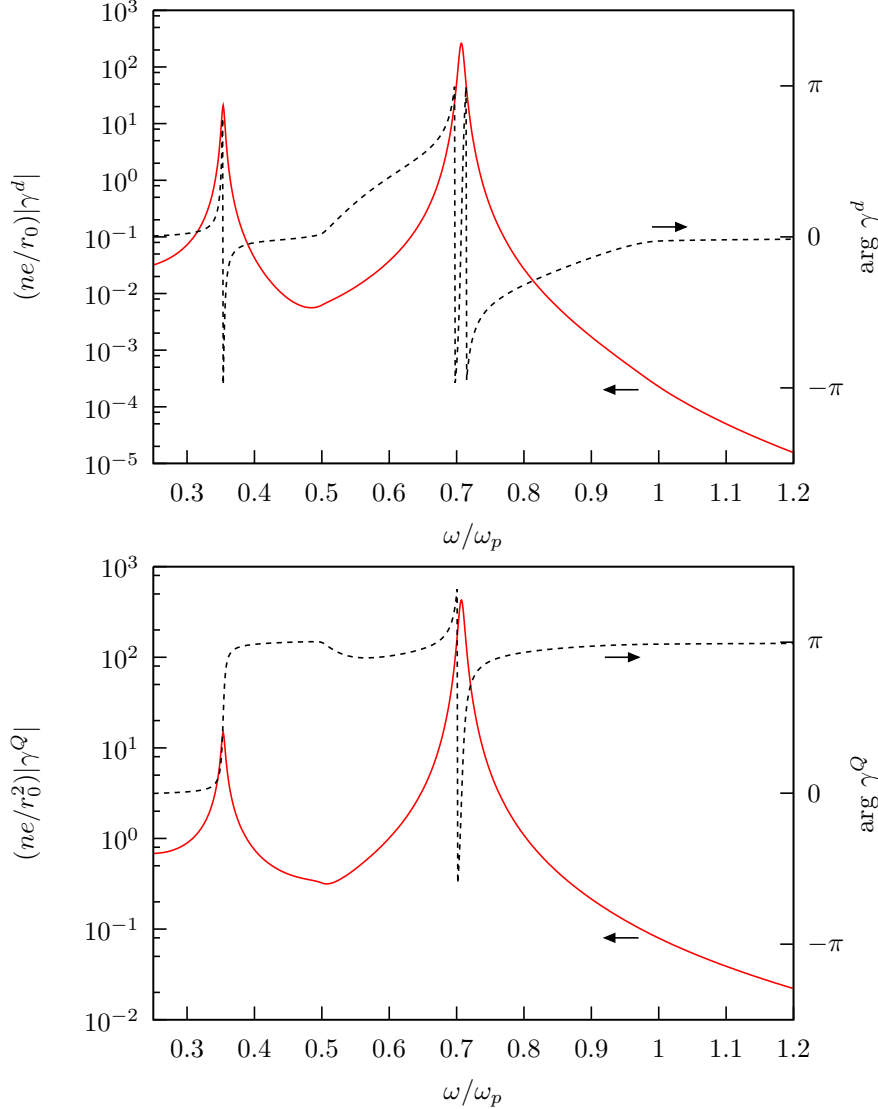


FIG. 3: Normalized absolute value (solid) and phase (dashed) of the dipolar (upper panel) and quadrupolar (lower panel) nonlinear response functions  $\gamma^d$  and  $\gamma^Q$  for a cylinder with deformation parameter  $d = 0.01$  made of a Drude metal as a function of the normalized frequency  $\omega/\omega_p$  (color online).

of the cylinder is small compared to the wavelength, so we may assume the incoming field to be constant within the particle and use the expressions obtained in the previous section corresponding to a homogeneous external field. Notice there is a competition between the dipolar and quadrupolar contributions to the radiation, and that their relative strength varies as the frequency increases. We remark that the SH dipole would be zero for the non-deformed cylinder, but for deformations as small as 1% its contribution to the radiation is comparable

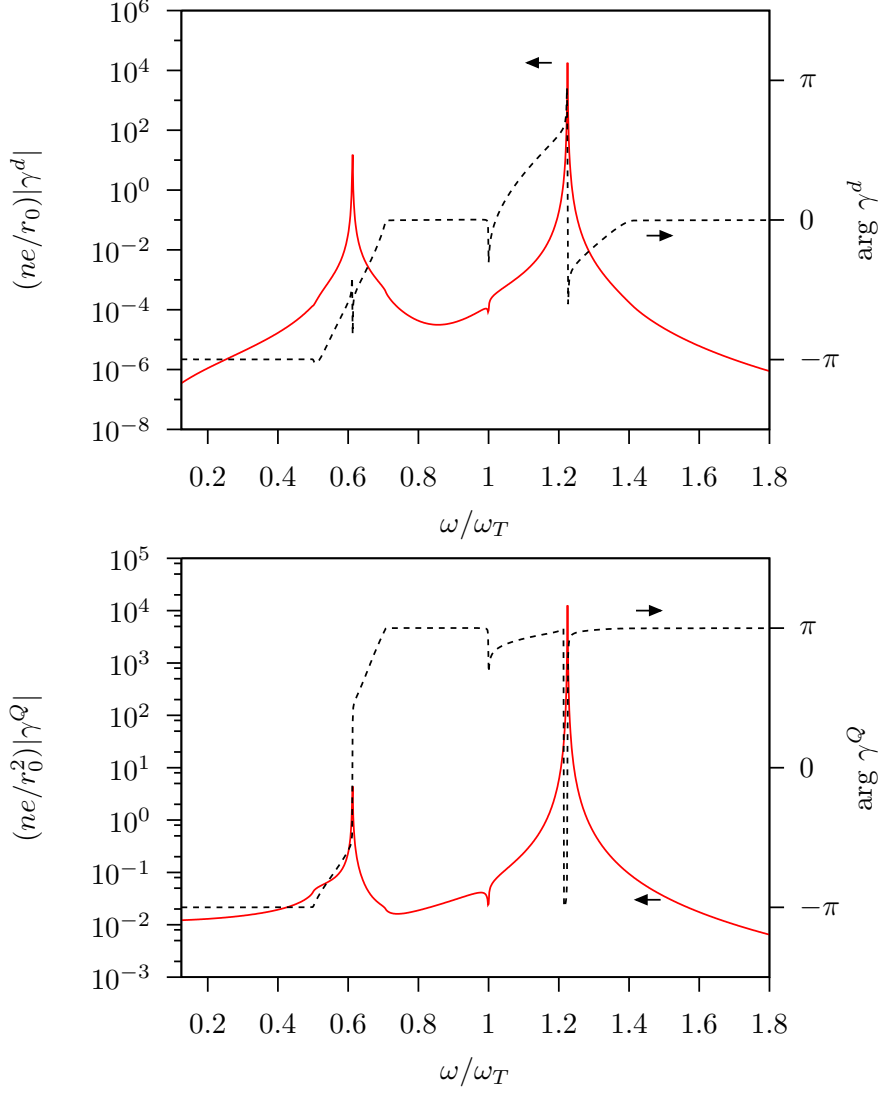


FIG. 4: Normalized absolute value (solid) and phase (dashed) of the dipolar (upper panel) and quadrupolar (lower panel) nonlinear response functions  $\gamma^d$  and  $\gamma^Q$  for a cylinder made of a dispersive dielectric with a Lorentzian resonance characterized by a longitudinal  $\omega_L$  and a transverse  $\omega_T$  frequency with  $\omega_L = \sqrt{2}\omega_T$ , and a deformation parameter  $d = 0.01$  as a function of the normalized frequency  $\omega/\omega_T$  (color online).

to the quadrupolar contribution. Fig. 5 shows that for low frequencies,  $\omega < \omega_{sp}/2$  displayed in the top left panel, the radiation is completely dominated by the dipolar term and it displays the typical pattern consisting of two symmetrical lobes. As the frequency moves towards the resonance the total radiated power increases hence the outermost curve in the top left panel corresponds to a frequency slightly below the resonance at  $\omega_{sp}/2$ . For higher

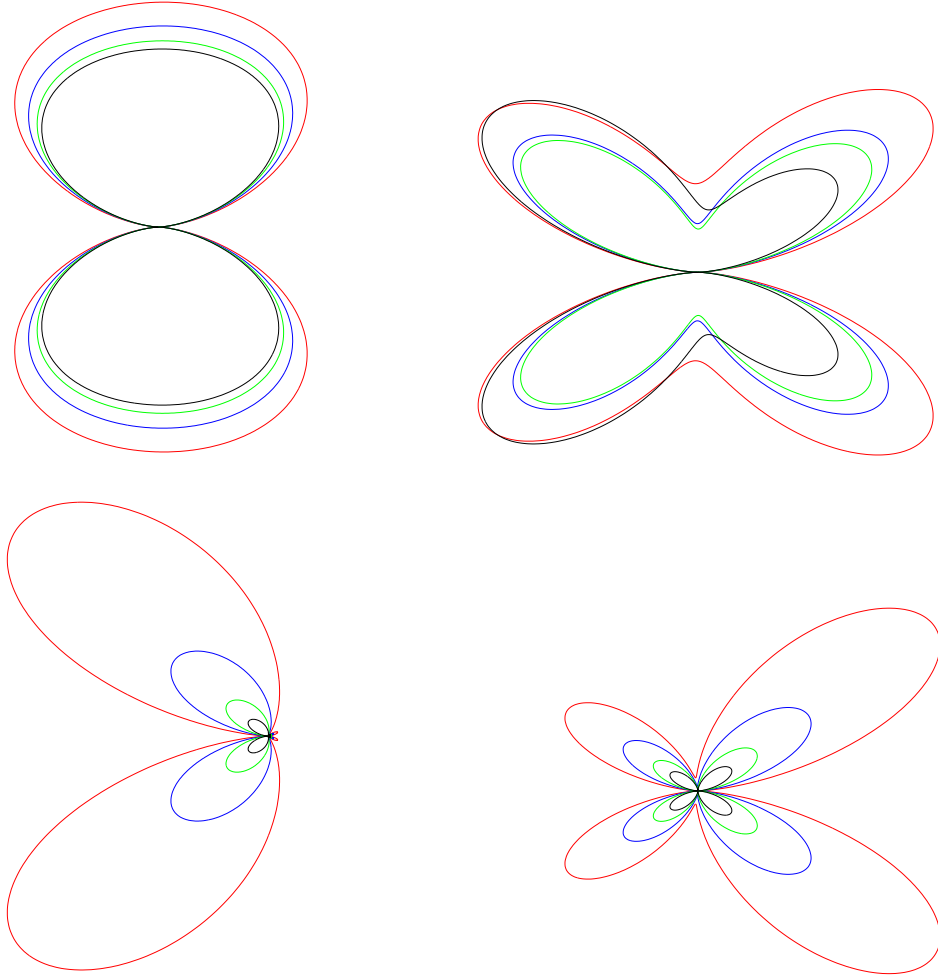


FIG. 5: Angular radiation pattern for a deformed metallic cylinder with deformation parameter  $d = 0.01$  described by a Drude response for frequencies  $\omega$  approaching  $\omega_{sp}$  or to its subharmonic:  $\omega < \omega_{sp}/2$  (upper left),  $\omega_{sp}/2 < \omega$  (upper right),  $\omega < \omega_{sp}$  (bottom left), and  $\omega > \omega_{sp}$  (bottom right). As  $\omega$  approaches a resonance curves the total radiated power increases (color online).

frequencies the pattern becomes largely quadrupolar. The top right panel corresponds to  $\omega > \omega_{sp}/2$  for which the quadrupolar contribution overshadows the dipolar contribution and a four lobed pattern emerges. It is somewhat asymmetrical due to the interference with the dipolar field. Also note the shift in the size of the lobes from front to back as one moves away from the resonance at  $\omega_{sp}/2$ . The bottom left panel illustrates the radiation pattern for frequencies approaching  $\omega_{sp}$  from below and is predominantly dipolar with an influence of the quadrupolar contribution which makes it asymmetrical. Radiation at frequencies above that of the surface plasmon  $\omega > \omega_{sp}$  is shown in the bottom right panel. In this region too,

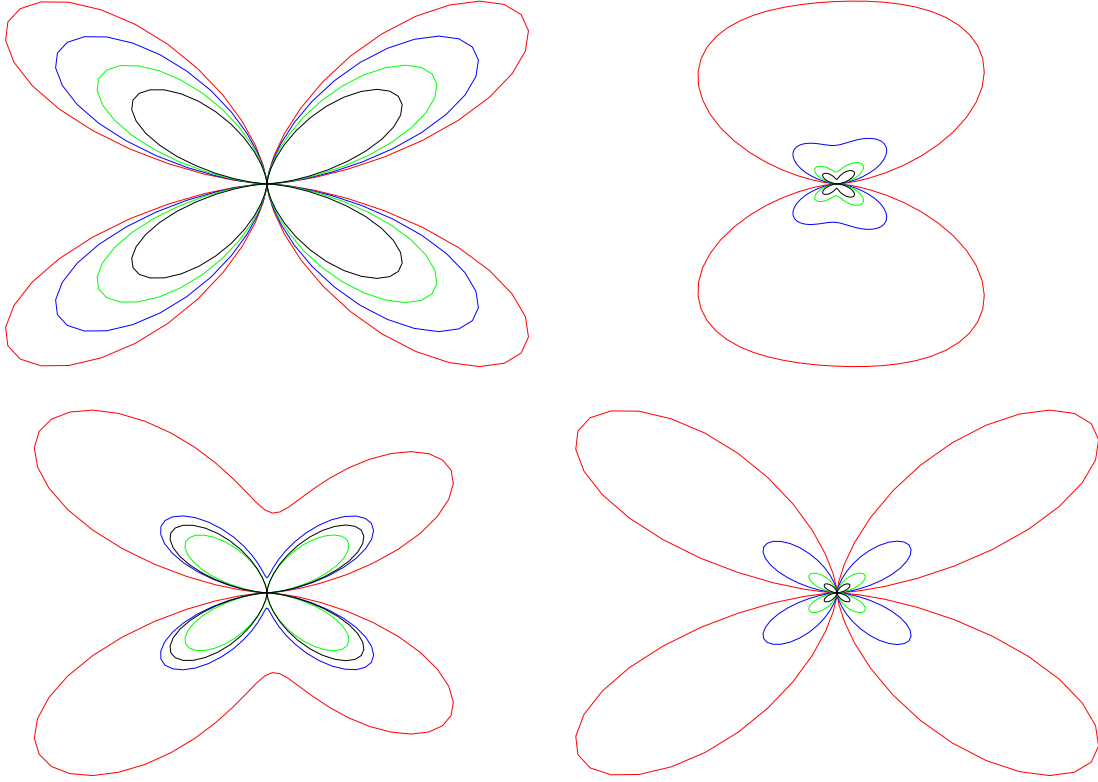


FIG. 6: Angular radiation pattern for a deformed dielectric cylinder with deformation parameter  $d = 0.01$  described by a simple Lorentzian response with negligible dissipation for frequencies  $\omega$  close to  $\omega_{spp}$  or its subharmonic:  $\omega < \omega_{spp}/2$  (upper left),  $\omega_{spp}/2 < \omega$  (upper right),  $\omega < \omega_{spp}$  (bottom left), and  $\omega > \omega_{spp}$  (bottom right). As  $\omega$  approaches a resonance the total radiated power increases (color online).

the pattern is mostly quadrupolar displaying four lobes which are asymmetrical due to the interference with the dipolar contribution to the radiation.

In Fig. 6 we show the SH angular radiation pattern as in Fig. 5 but corresponding to a dielectric particle as in Fig. 4. Here, we also see the competition between the dipolar and the quadrupolar radiation with the variation in frequency and the asymmetry in the different lobes of the quadrupolar pattern arising due to the phase difference between the two terms. Similar to Fig. 5, as the frequency approaches a resonance the total radiated power increases. However, the quadrupolar contribution to the radiation is stronger at lower frequencies in this case unlike the metallic case (Fig. 5). In the top left panel we plot the patterns for  $\omega < \omega_{spp}/2$  where the quadrupolar contribution to the radiation overshadows



the dipolar one and is therefore symmetric. The top right panel illustrates the radiation for frequencies  $\omega > \omega_{spp}/2$ . The outermost curve, closest and slightly above the resonance at  $\omega_{spp}/2$  displays a slightly distorted dipolar pattern. Moving away from the resonance, the quadrupolar term gets relatively stronger and the competition between the two terms gives rise to an asymmetry in the pattern. The bottom right panel shows the pattern for  $\omega < \omega_{spp}$  and it shows almost symmetrical quadrupolar patterns with the asymmetry appearing in the outermost curves, just below the resonance frequency. The bottom right panel shows the radiation at higher frequencies  $\omega > \omega_{spp}$  which is also symmetric and almost pure quadrupolar like radiation.

#### IV. CONCLUSIONS

We developed an analytical formalism to study the second order nonlinear optical response of isolated particles made of centrosymmetric materials with a cross-section slightly deformed away from that of a centrosymmetric particle. To this end, we choose the most simple geometry that lacks inversion symmetry, namely, a cylinder with an almost circular cross-section with three small protuberances separated by an angle of  $2\pi/3$ . We employed a perturbative approach choosing the extent of the deformation away from the symmetrical geometry as the smallness parameter. This allowed us to obtain simple closed form expressions for the electric fields within and beyond the particles and on their surfaces at both the fundamental and second harmonic (SH) frequencies. The self-consistent field near the surface of the particle was used to calculate the induced nonlinear polarization and the nonlinear hyperpolarizabilities. The zeroeth order term in the expansion corresponds to the case of a symmetric cylindrical particle yielding no SH dipole but a nonzero quadrupolar response. At the first order in the deformation the effect of a small deviation from centrosymmetrical geometry yields a dipolar contribution proportional to the deformation parameter which increases with the size of deformation and competes with that of the quadrupole already for very slightly deformed metallic and dielectric particles. We have only considered the dominant dipolar and quadrupolar contributions to the nonlinear hyperpolarizabilities in this work as the higher order multipoles generate a much weaker SH signal.

The dipolar and quadrupolar nonlinear responses were obtained in terms of the linear dielectric response of the material at the fundamental and SH frequencies and were found

to have resonant structures corresponding to the poles and zeroes of the dielectric function, and to the surface plasmon or surface plasmon-polariton frequencies of the undeformed particle, and to their subharmonics, as well as additional structure due to the normal nonlinear surface parameter  $a$ . We showed results for particles made up of a Drude metal and of a dielectric characterized by a simple Lorentzian response, as they allow a simple interpretation of the resulting spectra and radiation patterns. Nevertheless, as the input to our calculations are the dielectric functions of the particles, they may be applied to particles made of arbitrary materials for which  $\epsilon$  is known. Our approach can also be generalized to other geometries. Finally, we showed that the dipolar SH radiation is comparable and may overshadow the quadrupolar contribution for deformations as small as 1%. On the other hand, the dipolar hyperpolarizabilities (per unit length) reached at resonance values several orders of magnitude larger than  $r_0/ne$ , with  $r_0$  the nominal size of the particle,  $n$  the polarizable entity or the electronic number density and  $e$  the electronic charge (see Figs. 3 and 4). Thus, we expect that the dipolar nonlinear susceptibility of a metamaterial made up of these particles could be much larger than  $1/ner_0$ . As the typical susceptibility of non-centrosymmetric materials is of order  $1/nea_B$  with  $a_B$  the Bohr's radius, a metamaterial made of centrosymmetric materials with a non-centrosymmetric geometry may be a competitive source of SH provided  $a_B/r_0$  is not too small. Finally, we remark that our calculation of the nonlinear response of a particle showed that there are some subtleties to be accounted for: bulk contributions, bulk induced surface charges, surface originated surface charges and surface dipolar layers. All of these have to be appropriately screened to get consistent expressions for the hyperpolarizabilities. Analytical results for simple models that take all of these contributions into account are important in order to calibrate and test numerical calculations which may then, if proved to be correct, be applied to a larger class of systems. We expect that the present results will be useful for this purpose.

### Acknowledgments

This work was supported by DGAPA-UNAM under grants IN113016 and IN111119 (WLM) and by CONACyT (RS). We acknowledge useful talks with V. Agarwal, A. Reyes-Esqueda, L. Juárez-Reyes and B. Mendoza.

## Appendix

In this appendix we calculate the fields in the radiation zone due to localized systems of oscillating charge and current densities in 2D in order to obtain the corresponding angular radiation patterns. We will only consider electric dipole and quadrupole radiation. The treatment is predominantly similar to that of 3D<sup>23</sup>, but using the Green's function for the 2D wave equation and we follow Ref. 28.

We will consider a harmonically varying monochromatic current distribution  $\mathbf{J}(\mathbf{r}, t) = \mathbf{J}(\mathbf{r})e^{-i\omega t}$ . In the Lorentz gauge, the vector potential is also monochromatic and obeys a wave equation which becomes a Helmholtz equation for its amplitude  $\mathbf{A}(\mathbf{r})$  with a source  $-4\pi\mathbf{J}(\mathbf{r})/c$ . To solve it we first find the corresponding Green's function in 2D  $G(|\mathbf{r} - \mathbf{r}'|)$ , which obeys

$$(\nabla^2 + k^2)G(r) = -4\pi\delta(\mathbf{r}). \quad (\text{A.36})$$

Beyond the singularity,  $G(r)=R(kr)$ , where

$$s^2 \frac{d^2}{ds^2} R(s) + s \frac{d}{ds} R(s) + s^2 R(s) = 0. \quad (\text{A.37})$$

The solution is proportional to an outgoing Hankel function  $H_0^{(1)}(s)$ , which in the near zone, ( $s \rightarrow 0$ ), takes the form

$$\lim_{s \rightarrow 0} H_0^{(1)}(s) = 2i \log(s)/\pi. \quad (\text{A.38})$$

As the nonretarded Green's function in 2D is  $G = -2 \ln(r) + \text{constant}$ , a comparison with Eq.(A.38) yields  $G(r) = i\pi H_0^{(1)}(kr)$ . Thus, using the asymptotic expression for the Hankel's function for large arguments, we obtain in the radiation zone ( $kr \rightarrow \infty$ ),

$$G(r) = e^{i\pi/4} \sqrt{\frac{2\pi}{kr}} e^{ikr}. \quad (\text{A.39})$$

The retarded vector potential is then

$$\mathbf{A}(\mathbf{r}) = \frac{1}{c} \int d^2r' e^{i\pi/4} \sqrt{\frac{2\pi}{k|\mathbf{r} - \mathbf{r}'|}} e^{ik|\mathbf{r} - \mathbf{r}'|} \mathbf{J}(\mathbf{r}'), \quad (\text{A.40})$$

For a localized source in the long wavelength approximation  $r' \ll \lambda \ll r$  one can approximate Eq.(A.40) as

$$\mathbf{A}(\mathbf{r}) \approx \frac{1}{c} \sqrt{\frac{2\pi}{kr}} e^{i\pi/4} e^{ikr} \int d^2r' \mathbf{J}(\mathbf{r}') \sum_{m=0} \frac{(-ik)^m}{m!} (\hat{\mathbf{r}} \cdot \mathbf{r}')^m. \quad (\text{A.41})$$

The first term ( $m = 0$ ) in the series (A.41) may be integrated to obtain the dipolar contribution to the potential,

$$\mathbf{A}^{(0)} = (-ie^{i\pi/4})\sqrt{2\pi}\sqrt{\frac{k}{r}}e^{ikr}\mathbf{p}, \quad (\text{A.42})$$

where  $\mathbf{p}$  is the amplitude of the oscillating dipole moment per unit length. The second term ( $m = 1$ ) is

$$\mathbf{A}^{(1)}(\mathbf{r}) = \frac{1}{c}\sqrt{\frac{2\pi}{kr}}e^{i\pi/4}e^{ikr}(-ik)\int d^2r'\mathbf{J}(\mathbf{r}')(\hat{\mathbf{r}}\cdot\mathbf{r}'). \quad (\text{A.43})$$

Within the integral we can write  $\mathbf{J}(\mathbf{r}')(\hat{\mathbf{r}}\cdot\mathbf{r}') = (1/2)[\mathbf{J}(\mathbf{r}')(\hat{\mathbf{r}}\cdot\mathbf{r}') + \mathbf{r}'(\hat{\mathbf{r}}\cdot\mathbf{J}(\mathbf{r}'))] + (1/2)[\mathbf{J}(\mathbf{r}')(\hat{\mathbf{r}}\cdot\mathbf{r}') - \mathbf{r}'(\hat{\mathbf{r}}\cdot\mathbf{J}(\mathbf{r}'))]$  as a sum of a symmetric and an antisymmetric part. The former can be manipulated to yield

$$\mathbf{A}^{(1s)}(\mathbf{r}) = (\sqrt{2\pi}e^{i\pi/4})\frac{e^{ikr}}{4\sqrt{r}}k^{3/2}\mathbf{Q}\cdot\hat{\mathbf{r}}, \quad (\text{A.44})$$

where  $\mathbf{Q}$  is the 2D quadrupolar tensor (Eq. (3)). The antisymmetric part yields the magnetic dipolar radiation.

As usual, we may obtain the electromagnetic radiation field as  $\mathbf{B} = \nabla \times \mathbf{A} \approx ik\hat{\mathbf{r}} \times \mathbf{A}$  and  $\mathbf{E} = \mathbf{B} \times \hat{\mathbf{r}}$ , so that from Eqs. (A.42) and (A.44) we obtain Eqs. (32) and (33).

- 
- <sup>1</sup> Daria Smirnova and Yuri S. Kivshar. Multipolar nonlinear nanophotonics. *Optica*, 3(11):1241–1255, Nov 2016.
  - <sup>2</sup> Yu-xi Zhang and Yu-hua Wang. Nonlinear optical properties of metal nanoparticles: a review. *RSC Adv.*, 7:45129–45144, 2017.
  - <sup>3</sup> Vera L. Brudny, Bernardo S. Mendoza, and W. Luis Mochán. Second-harmonic generation from spherical particles. *Phys. Rev. B*, 62:11152–11162, Oct 2000.
  - <sup>4</sup> Bingzhong Huo, Xianghui Wang, Shengjiang Chang, and Ming Zeng. Second harmonic generation of a single centrosymmetric nanosphere illuminated by tightly focused cylindrical vector beams. *J. Opt. Soc. Am. B*, 29(7):1631–1640, Jul 2012.
  - <sup>5</sup> Jing-Wei Sun, Xiang-Hui Wang, Sheng-Jiang Chang, Ming Zeng, and Na Zhang. Second harmonic generation of metal nanoparticles under tightly focused illumination. *Chinese Physics B*, 25(3):37803, 2016.

- <sup>6</sup> Brian K. Canfield, Hannu Husu, Janne Laukkanen, Benfeng Bai, Markku Kuittinen, Jari Turunen, and Martti Kauranen. Local field asymmetry drives second-harmonic generation in noncentrosymmetric nanodimers. *Nano Letters*, 7(5):1251–1255, 2007.
- <sup>7</sup> Sinjeung Park, Jae W. Hahn, and Jae Yong Lee. Doubly resonant metallic nanostructure for high conversion efficiency of second harmonic generation. *Opt. Express*, 20(5):4856–4870, Feb 2012.
- <sup>8</sup> J. Butet, G. Bachelier, I. Russier-Antoine, F. Bertorelle, A. Mosset, N. Lascoux, C. Jonin, E. Benichou, and P.-F. Brevet. Nonlinear fano profiles in the optical second-harmonic generation from silver nanoparticles. *Phys. Rev. B*, 86:075430, Aug 2012.
- <sup>9</sup> Renlong Zhou, Hua Lu, Xueming Liu, Yongkang Gong, and Dong Mao. Second-harmonic generation from a periodic array of noncentrosymmetric nanoholes. *J. Opt. Soc. Am. B*, 27(11):2405–2409, Nov 2010.
- <sup>10</sup> W. L. Schaich. Second harmonic generation by periodically-structured metal surfaces. *Phys. Rev. B*, 78:195416, Nov 2008.
- <sup>11</sup> Jerry I. Dadap, Jie Shan, and Tony F. Heinz. Theory of optical second-harmonic generation from a sphere of centrosymmetric material: small-particle limit. *J. Opt. Soc. Am. B*, 21(7):1328–1347, Jul 2004.
- <sup>12</sup> Jerry Icban Dadap. Optical second-harmonic scattering from cylindrical particles. *Phys. Rev. B*, 78:205322, Nov 2008.
- <sup>13</sup> Alex G. F. de Beer and Sylvie Roke. Nonlinear mie theory for second-harmonic and sum-frequency scattering. *Phys. Rev. B*, 79:155420, Apr 2009.
- <sup>14</sup> Antonio Capretti, Carlo Forestiere, Luca Dal Negro, and Giovanni Miano. Full-wave analytical solution of second-harmonic generation in metal nanospheres. *Plasmonics*, 9(1):151–166, Feb 2014.
- <sup>15</sup> Naveen K. Balla, Peter T. C. So, and Colin J. R. Sheppard. Second harmonic scattering from small particles using discrete dipole approximation. *Opt. Express*, 18(21):21603–21611, Oct 2010.
- <sup>16</sup> Guillaume Bachelier, Isabelle Russier-Antoine, Emmanuel Benichou, Christian Jonin, and Pierre-François Brevet. Multipolar second-harmonic generation in noble metal nanoparticles. *J. Opt. Soc. Am. B*, 25(6):955–960, Jun 2008.
- <sup>17</sup> Jérémy Butet and Olivier J. F. Martin. Evaluation of the nonlinear response of plasmonic

- metasurfaces: Miller's rule, nonlinear effective susceptibility method, and full-wave computation. *J. Opt. Soc. Am. B*, 33(2):A8–A15, Feb 2016.
- <sup>18</sup> J r my Butet, Benjamin Gallinet, Krishnan Thyagarajan, and Olivier J. F. Martin. Second-harmonic generation from periodic arrays of arbitrary shape plasmonic nanostructures: a surface integral approach. *J. Opt. Soc. Am. B*, 30(11):2970–2979, Nov 2013.
- <sup>19</sup> Carlo Forestiere, Antonio Capretti, and Giovanni Miano. Surface integral method for second harmonic generation in metal nanoparticles including both local-surface and nonlocal-bulk sources. *J. Opt. Soc. Am. B*, 30(9):2355–2364, Sep 2013.
- <sup>20</sup> Lei Zhang, Shifei Tao, Zhenhong Fan, and Rushan Chen. Efficient method for evaluation of second-harmonic generation by surface integral equation. *Opt. Express*, 25(23):28010–28021, Nov 2017.
- <sup>21</sup> Gabriel D. Bernasconi, J r my Butet, and Olivier J. F. Martin. Mode analysis of second-harmonic generation in plasmonic nanostructures. *J. Opt. Soc. Am. B*, 33(4):768–779, Apr 2016.
- <sup>22</sup> Ulises R. Meza, Bernardo S. Mendoza, and W. Luis Moch n. Second-harmonic generation in nano-structured metamaterials. submitted to *Phys. Rev. B*, Dec. 2018.
- <sup>23</sup> John David Jackson. *Classical electrodynamics; 2nd ed.* Wiley, New York, NY, 1975.
- <sup>24</sup> Bernardo S. Mendoza and W. Luis Moch n. Exactly solvable model of surface second-harmonic generation. *Phys. Rev. B*, 53:4999–5006, Feb 1996.
- <sup>25</sup> Joseph Rudnick and E. A. Stern. Second-harmonic radiation from metal surfaces. *Phys. Rev. B*, 4:4274–4290, Dec 1971.
- <sup>26</sup> N.W. Ashcroft and N.D. Mermin. *Solid State Physics*. Saunders College, Philadelphia, 1976.
- <sup>27</sup> Jes s A. Maytorena, Bernardo S. Mendoza, and W. Luis Moch n. Theory of surface sum frequency generation spectroscopy. *Phys. Rev. B*, 57:2569–2579, Jan 1998.
- <sup>28</sup> Raksha Singla and W. Luis Moch n. Multipolar radiation in 2d. In preparation.